Research Square

Preprints are preliminary reports that have not undergone peer review.
They should not be considered conclusive, used to inform clinical practice,
or referenced by the media as validated information.

Stronger HBc-specific B cell activity in chronic HBV-infected children with higher liver inflammatory grade and better antiviral therapy response

Yingzhi Zhou

1812313752@qq.com

Chongqing Medical University https://orcid.org/0000-0002-9266-6744

Jiangtao He

Chongqing Medical University

Huasi Wang

Chongqing Medical University

Kai Zhu

Chongqing Medical University

Jiaying Wu

Chongqing Medical University

Yunan Chang

Chongqing Medical University

Dachuan Cai

Chongqing Medical University

Hong Ren

Chongqing Medical University

Hongmei Xu

Chongqing Medical University

Min Chen

Chongqing Medical University https://orcid.org/0000-0002-9996-5149

Research Article

Keywords: Chronic Hepatitis B, Children, Hepatic transcriptome, HBc-specific B cells, Anti-viral treatment

Posted Date: June 5th, 2026

DOI: https://doi.org/10.21203/rs.3.rs-9678329/v1

License: This work is licensed under a Creative Commons Attribution 4.0 International License.
Read Full License

Abstract

Background

Although the majority of children with chronic HBV infection (CHB) are asymptomatic and in the immune tolerance phase, some of them develop progressive liver disease. The mechanisms of the progression of liver disease in these CHB children remain largely unclear.

Methods

20 CHB children were enrolled for comparison of hepatic transcriptome profiles between no-significant and significant liver inflammation, and analysis of the correlations between the hepatic gene expression and clinical parameters or anti-viral responses. Quantity, phenotype and function of peripheral B cell and HBc-specific B (HBc-B) cells were assessed in another 97 treatment-naïve CHB children during different clinical phases, in which 17 subsequently receiving ETV treatment for analysis of longitudinal changes in the peripheral HBc-B cells and their relationship to anti-viral responses.

Results

Bioinformatic analysis and liver biopsy staining revealed that remarkably enhanced hepatic B cell infiltration was the distinctive feature of CHB children with significant liver inflammation. Dramatically increased peripheral HBc-B cell frequency, HBcAb-secreting spot-forming cell (HBcAb SFC) count, and serum HBcAb level were observed in CHB children during immune active phase. HBcAb SFC count and HBcAb level were significantly positively correlated to liver inflammation grade or ALT level. Higher hepatic level of B cell-related genes, elevated percentage of peripheral HBc-B cell, and raised level of serum HBcAb were found in CHB children with more HBeAg decline at week 12 or 48 of ETV treatment.

Conclusion

Higher activity of HBc-B cells would be linked to increased liver inflammation and more favorable antiviral treatment outcomes in pediatric CHB patients.

Study highlights

- Significant hepatic B cell infiltration was the distinctive feature of CHB children with significant liver inflammation.
- Significantly higher frequency of peripheral HBc-B cells, HBcAb-secreting spot-forming cell (HBcAb SFC) count, and serum HBcAb level in CHB children during immune active phase.

- Peripheral HBcAb SFC count or serum HBcAb level was significantly positively correlated to liver inflammation grade or ALT level.
- Higher hepatic levels of B cell-related genes, higher percentage of peripheral HBc-B cell or level of serum HBcAb in CHB children with more HBeAg decline at week 12 or 48 of ETV treatment.

Introduction

Although the widespread implementation of infant hepatitis B vaccination over the past four decades has significantly reduced the number of new infections in children, nearly 2 million children under the age of 5 still acquire hepatitis B virus (HBV) infection each year, primarily through mother-to-child transmission and early childhood horizontal transmission[1,2]. Traditionally, it has been believed that pediatric patients with chronic HBV infection (CHB) are predominantly in an immune tolerance phase with normal ALT levels, and no-significant liver inflammation or liver disease progression[3]. Zhu et al. have indicated that approximately 90% of pediatric patients clinically diagnosed with immune-tolerant CHB exhibit some degree of hepatic inflammatory activity and/or fibrosis, with the prevalence of severe liver fibrosis and cirrhosis reaching up to 10.9%[4]. Furthermore, several long-term cohort studies conducted in earlier years have reported that children with CHB remain at risk of developing hepatocellular carcinoma (HCC)[5,6]. These findings underscore the need for greater attention to disease progression monitoring and therapeutic strategies in children and adolescents with chronic HBV infection.

CHB is a dynamic disease characterized by multiple clinical phases, which are defined based on HBV DNA levels, HBeAg status, ALT levels, and the degree of hepatic inflammation and necrosis. These phases include the immune-tolerant (IT) phase, immune-active (IA) phase, immune-control (IC) phase, and reactivation phase[7]. During the course of hepatitis B infection, HBV itself is not directly cytopathic to hepatocytes. Rather, hepatocellular injury and hepatic inflammation are predominantly mediated by virus-specific host immune responses mounted to eradicate the infection. Sustained immune-mediated inflammation represents a central pathogenic mechanism driving the progression of liver fibrosis, ultimately leading to cirrhosis and the development of HCC[8]. Chronic HBV infection in pediatric patients presents unique challenges due to its diverse clinical manifestations and evolving immunopathological characteristics. At present, studies investigating the progression of hepatitis in children are limited and are predominantly focused on peripheral immune characteristics. Zhang et al. demonstrated that intrahepatic infiltration of dendritic cells (DCs) in CHB children positively correlated with serum ALT levels and negatively correlated with HBV viral load. Interestingly, peripheral DC frequency was significantly reduced in patients with elevated ALT levels[9]. Our previous study also showed significant activation of peripheral natural killer (NK) cells and T cells in pediatric CHB patients, particularly during the IA phase[10].

In addition, HBV-specific immune responses played a crucial role in the progression and clinical outcomes of CHB. HBV-specific T cells are characterized by reduced frequency and impaired functionality in chronic HBV infection[11]. A study demonstrated that HBsAg reduction was associated

with hepatitis B core-specific CD8 T cell quality[12]. Patients with HBsAg levels < 500 IU/mL exhibited significantly stronger HBsAg-specific CD4 + T-cell responses compared with those with HBsAg levels ≥ 500 IU/mL[13]. It has been reported that patients with high frequencies of HBV core- and polymerase-specific T cells were able to maintain sustained control of HBV after nucleos(t)ide analogue (NUC) discontinuation, with a low incidence of hepatitis relapse[14]. HBcAg, functioning as both a T cell–dependent and T cell–independent antigen, is capable of eliciting robust HBV-specific immune responses. A recent study demonstrated that HBcAg-specific B cells were present at a higher frequency than HBsAg-specific B cells in patients with CHB. Transcriptomic profiling of HBsAg- and HBcAg-specific B cells from these patients suggested that HBV-specific B cells may exert additional functions beyond antibody production[15]. However, data on HBV-specific immune responses in children remain limited. Recent studies have indicated that HBV-specific T-cell responses were not correlated with serum HBsAg levels, whereas patient age, potentially reflecting the duration of infection, was a key determinant of the frequency of HBsAg-specific T cells[16,17]. Kennedy found that younger patients exhibited a higher frequency of HBV-specific T cells with proliferative and cytokine-producing capacity compared to older adult CHB patients[18].

Intrahepatic immune profiles more accurately reflect the true immunological status of patients with CHB and provide more meaningful prognostic information regarding disease progression and therapeutic outcomes. In recent years, transcriptomic analysis has emerged as a powerful tool for revealing the complex mechanisms of hepatic inflammation. Currently, limited data on intrahepatic immune features of CHB mainly focus on adult patients[19,20], with much less clarity in pediatric patients.

Current evidence suggests that the immune response is associated with the efficacy of antiviral therapy[21,22]. Despite significant advances in antiviral therapy in CHB children[23–25], the interplay between host immune responses and disease progression remains insufficiently understood. Zhang et al. found that the frequency and function of peripheral plasmacytoid dendritic cells (pDCs) were associated with IFN-α treatment response[26]. In addition, restoration of peripheral HBcAg-specific T cells in children with CHB was associated with a reduction in HBV viral load during antiviral therapy[27]. Consequently, identifying immune factors associated with disease progression in children with chronic hepatitis B could help optimize treatment strategies.

Therefore, this study performed transcriptomic profiling of liver tissues and explored characteristics of corresponding peripheral immune cells from children with chronic HBV infection, aiming to elucidate the immunological mechanisms underlying liver disease progression in children and to discover immune factors associated with the efficacy of antiviral therapy.

Materials and methods

Patients

Twenty HBeAg-positive CHB children who completed pre-treatment liver histological examination were included as Cohort 1 for exploring liver tissue transcriptomic expression profiling. Among these 20 patients, 14 received ETV therapy and completed 48 weeks of follow-up. Another 97 treatment-naïve children with chronic HBV infection were enrolled as Cohort 2 for analysis of baseline peripheral global and HBV-specific B cells. Of these 97 CHB children, 17 received ETV therapy and 14 completed 48 weeks of follow-up (3 lost to follow-up after 24 weeks). According to the Chinese Guidelines for the Prevention and Treatment of Chronic Hepatitis B[7], these 97 CHB patients were categorized into the IT phase (n = 49), IA phase (n = 40), and IC phase (n = 8). The summary of patient enrollment and follow-up was in the flowchart provided in Supplementary Fig. 1. Written informed consent was obtained from all participants and their guardians. The study protocol was approved by the Ethics Committee of Children's Hospital of Chongqing Medical University and conducted in accordance with the guidelines of the Declaration of Helsinki.

Clinical and virological parameters

Blood samples from the enrolled pediatric patients were analyzed at the Clinical Laboratory Center of our hospital. Hematological analysis, biochemical testing, HBV serological markers, and quantitative HBV DNA measurements were performed. Biochemical parameters were measured using standard automated analyzers. Serum HBV DNA levels were quantified by quantitative real-time polymerase chain reaction (qPCR), with a lower limit of quantitation (LLOQ) of 400 IU/mL. HBV serological markers were detected using a chemiluminescent microparticle immunoassay kit (Abbott GmbH & Co. KG, Germany). The LLOQ for HBsAg was 0.05 IU/mL. Quantitative levels of serum HBcAb were measured using a double-antigen sandwich immunoassay (Wantai, Beijing, China).

Histopathological diagnosis of liver tissue

Histopathological diagnosis of liver tissue was conducted jointly by two experienced pathologists at our hospital. The degree of hepatic inflammation (Grade, G) and the stage of fibrosis (Stage, S) were assessed according to the Scheuer scoring system, with scores ranging from 0 to 4. The grade of necroinflammatory activity was classified as G0 (none), G1 (mild), G2 (mild to moderate), G3 (moderate), and G4 (severe). And the stage of fibrosis was classified as S0 (no fibrosis), S1 (minimal fibrosis), S2 (moderate fibrosis), S3 (severe fibrosis), and S4 (cirrhosis). Significant liver inflammation or fibrosis was defined as a Scheuer score more than or equal to G2 or S2. Discrepancies between pathologists were resolved through consensus review with a third senior pathologist.

Immunohistochemistry

Following dehydration, tissue sections were incubated with 3% hydrogen peroxide solution at room temperature for 15 min. Antigen retrieval was performed using 0.01 M sodium citrate buffer under heat

induction, followed by blocking with 10% normal goat serum. The sections were then incubated overnight at 4°C with primary antibodies diluted in blocking buffer. A monoclonal mouse anti-human CD20 antibody (clone L26) was obtained from MXB Biotechnologies (Fuzhou, China). A ready-to-use biotinylated goat anti-human IgG secondary antibody was applied to bind the primary antibody. Finally, target proteins were visualized using avidin-labeled horseradish peroxidase and diaminobenzidine (DAB) staining (MXB Biotechnologies, Fuzhou, China). Stained slides were digitally scanned at 40× magnification using a 3DHISTECH whole-slide scanner.

Fluorescently labeled HBcAg

Recombinant HBcAg (genotype A, Bioforce Biotechnology, Bejing, China) was purchased from Bioforce Biotechnology. For labeling, purified recombinant HBcAg proteins were individually conjugated with DyLight™ 488 and DyLight™ 650 (Thermo Scientific, Waltham, MA, USA), and free unbound dye was removed using a dye removal resin column according to the manufacturer's instructions.

PBMCs thawing and flow cytometry analysis of total and HBcAg-specific B cells

Frozen PBMCs were quickly thawed in a 37°C water bath and immediately transferred to pre-warmed culture medium for washing and recovery, then PBMCs were incubated overnight in complete RPMI 1640 medium supplemented with 10% fetal bovine serum (FBS) and 1% penicillin-streptomycin at 37°C with 5% CO_2 to allow recovery. For B cell phenotypic analysis, PBMCs were stained with specific fluorochrome-conjugated monoclonal antibodies (mAbs), including HBcAg-D448 and -D650 (650 ng/mL), anti-CD3-PerCP5.5 (Biolegend, USA), anti-CD19-PE (Biolegend, USA), anti-CD27-PECy7 (Biolegend, USA), and anti-CD21-PE/Dazzle™594 (Biolegend, USA), and Zombie Aqua viability dye (Biolegend, USA). Intracellular IL-10-PE (Biolegend, USA), and IL-6-PerCP5.5 (Biolegend, USA) were detected after R848 (1 ug/mL, MCE, China) and Brefeldin A and Monensin mixture (250×, Lianke Biotechnology, Guangzhou, China) at 37℃ for 6 h. Multiparameter flow cytometry was performed using a CytoFLEX flow cytometer (Beckman Coulter, USA), and data were analyzed using FlowJo software (10.0.7r2, Treestar).

ELISpot for functional analysis of HBcAg-specific B cells in vitro

ELISPOT assays were performed as previously described with modifications[28]. Cryopreserved PBMCs were recovered in 24-well plates (2×10^6 cells/well) and cultured for 5 days at 37 ℃ in the presence of 10 ng/mL IL-2 (PeproTech, USA) and 1 μg/mL R848 (MCE, China). Viable cells were counted using trypan blue staining. Round-bottom 96-well ELISPOT plates were coated overnight (18 h) at 4 ℃ with 50 μL per well of 10 μg/mL HBcAg (Bioforce Biotechnology, Beijing, China) in PBS. Control wells were coated with anti-human IgG antibody according to the manufacturer's instructions (U-CyTech, Utrecht, The Netherlands), and wells coated with PBS alone served as background controls. Stimulated PBMCs were seeded in triplicate as follows: 200,000 viable cells per well for PBS-coated and HBcAg-coated wells, and

20,000 viable cells per well for anti-human IgG-coated wells. Cells were incubated for an additional 18 h at 37 ℃. IgG spot-forming cells (SFCs) were then developed following the kit protocol (U-CyTech, Utrecht, The Netherlands) and counted using a BioReader ELISpot reader (AID, Germany).

RNA sequencing and raw data processing

Liver tissues from CHB children were frozen immediately in liquid nitrogen. Total RNA was extracted using TRIzol reagent (Life Technologies, California, USA) following the manufacturer's instructions. Total RNA was extracted, and RNA quality was assessed using the Agilent Bioanalyzer 2100. Samples with the RNA 28S/18S ratio higher than 1.1 and the RNA Integrity Number (RIN) higher than 7.5 were used for further RNA sequencing. RNA sequencing was performed on the BGI DNBSEQ platform. Raw reads were filtered using SOAPnuke and clean reads were obtained and stored in FASTQ format. HISAT (Hierarchical Indexing for Spliced Alignment of Transcripts) was applied to align the clean reads to the human reference genome (GRCh38.p13).

Bioinformatics analysis of gene expression profiles

The differentially expressed genes (DEGs) were identified using the R package DESeq2[29]. DEGs with $P < 0.05$, false discovery rate (FDR) < 0.2, and $|\log_2 \text{fold change}| \geq 1$ were considered statistically significant. Gene Ontology (GO) enrichment analysis of DEGs were performed using the OECloud tools at https://cloud.oebiotech.com. Enrichment score of B cells was identified by immune infiltration analysis using ssGSEA according to Bindea' study[30].

Statistical analysis

Statistical analysis and data visualization were performed using SPSS version 25.0, GraphPad Prism 8, Origin 2021, and R software (version 4.1.3). For continuous variables, data were presented as median and interquartile range (IQR). The Mann-Whitney U test or Kruskal-Wallis test was used for comparisons between two or more independent groups, while the Wilcoxon signed-rank test was used for paired samples. Spearman's rank correlation was applied for correlation analysis. In this study, the strength of correlation was interpreted as follows: |related coefficient (RC)| < 0.4 indicated a weak correlation, 0.4–0.6 a moderate correlation, and ≥ 0.6 a strong correlation. For categorical variables, data were expressed as percentages, and comparisons between groups were conducted using the chi-square test or Fisher's exact test, as appropriate. Dunnett's test was applied for correction in multiple comparisons. All statistical inferences were based on two-tailed tests, and a P value < 0.05 was considered statistically significant.

Results

Hepatic transcriptome analysis revealed upregulated B cell-related pathway and genes in CHB children with significant liver inflammation

Total 20 CHB children were included in hepatic transcriptome analysis (Cohort 1), 7 children had moderate-to-severe liver necroinflammation (G2-3) and 13 children had no-activity or minimal liver necroinflammation (G0-1). The baseline characteristics of the two groups were shown in Table 1. These two groups had similar age and sex distribution, blood cell count, total bilirubin level, HBsAg level and HBV DNA load ($P > 0.05$). The ALT and AST levels in the G2-3 group were significantly higher than those in the G0-1 group ($P < 0.05$). HBsAg levels tended to be lower in the G2-3 group compared to the G0-1 group, although the difference was not statistically significant.

Table 1
The baseline characteristics of CHB children included in liver transcriptome analysis

Variables	**G0-1 (n = 13)**	**G2-3 (n = 7)**	***P* value**
Age (years)	9(3–12)	7(4–10)	0.748
Sex (boy, n (%))	4(30.8%)	4(57.1%)	0.356
WBC (10^9/L)	5.77(5.46–6.92)	5.26(4.85–6.77)	0.405
NEUT (10^9/L)	2.47(2.34–3.17)	3.17(2.17–3.18)	0.781
LY (10^9/L)	2.79(2.30–3.19)	2.65(2.14–2.92)	0.721
Mo(10^9/L)	0.30(0.25–0.34)	0.34(0.32–0.41)	0.164
PLT (10^9/L)	234.00(197.00-259.00)	247.00(213.50–260.00)	0.782
ALT (U/L)	81.00(45.00-162.00)	182.00(83.00-371.00)	0.047
AST (U/L)	77.00(42.00–90.00)	138.00(84.50–203.00)	0.029
TBIL (μmol/L)	8.00(6.00-10.80)	10.00(6.60–12.50)	0.525
HBsAg (log_{10} IU/mL)	4.32(4.08–4.69)	4.02(2.90–4.35)	0.091
HBV DNA (log_{10} IU/mL)	8.11(7.60–8.41)	7.56(7.18–8.07)	0.165
Data are presented as the median and interquartile range (IQR), or numbers with percentages (%).			
WBC, white blood cells; NEUT, neutrophils; LY, lymphocytes; Mo, monocytes; PLT, platelet; ALT, alanine aminotransferase; AST, aspartate transaminase; TBIL, total bilirubin; HBsAg, Hepatitis B surface antigen; HBV, hepatitis B virus; IU, international unit			

Firstly, the hepatic transcriptomic signatures were compared between G2-3 and G0-1 group for identification of DEGs. As shown in Fig. 1A, a total of 93 DEGs (55 upregulated and 38 downregulated genes) were identified in G2-3 group versus G0-1 group ($P < 0.05$, FDR < 0.2, and $|log_2FC| \geq 1$). Then, pathway enrichment analysis of DEGs was performed using Gene Ontology Biological Process (GOBP). The top 10 significantly enriched GO terms for upregulated or downregulated DEGs were presented in Fig. 1B, with ascending order of their P values. The results showed that the top 10 significantly enriched GO terms of the upregulated DEGs were related to "B cell receptor signaling pathway", "adaptive immune

response", "B cell activation", and "humoral immune response". And the most significantly enriched GO terms of downregulated DEGs included "sympathetic nervous system development", "positive regulation of neurogenesis", "long-term memory", and "response to retinoic acid".

Given that the most significantly upregulated processes in G2-3 group were associated to B cells, we further assessed the level of intrahepatic infiltration of B cell subsets. Enrichment scores of activated B cell, immature B cell, and memory B cell were calculated, using single-sample gene set enrichment analysis (ssGSEA) based on the expression levels of signature genes of different B cell subsets. As displayed in Fig. 1C, enrichment scores of activated B cell (-0.05 vs. -0.14, P = 0.037) and immature B cell (0.18 vs. 0.11, P = 0.009) were significantly higher in the G2-3 group. Besides, genes essential for B cell antigen receptor expression and function, such as MS4A1, CXCR5, and CD19, were significantly upregulated in the G2-3 group (P < 0.05), in which expression of MS4A1 (encoding CD20, marker for B cells) was upregulated most significantly. Immunohistochemistry staining of MS4A1 (CD20) also verified increased B cell number at the site of inflammatory cell infiltration in G2-3 group **(**Fig. 1D & 1E). Furthermore, expression levels of B cell-related genes, such as MS4A1, BANK1, CR1, FCGR1A, KLHL6, and GCSAM were also significantly positively correlated with ALT (P < 0.05, Fig. 1F). However, no significant correlation was found with viral indicators except for FCGR1A.

Higher hepatic active B-cell infiltration and B cell-related gene expression in CHB children with a better antiviral response

Among these 20 CHB children included in the hepatic transcriptome analysis (Cohort 1), 14 had received ETV antiviral therapy and completed 48 weeks of follow-up. Laboratory parameters at baseline and at 48 weeks of follow-up were shown in **Supplementary table 1**. Treatment response was defined based on the reduction in HBeAg or HBsAg levels at week 48. Patients were categorized into the following groups: HBeAg B (HBeAg decline < 1 $\log_{10}$ s/co), HBeAg G (HBeAg decline > 1 $\log_{10}$ s/co), HBsAg B (HBsAg decline < 1 $\log_{10}$ IU/mL), and HBsAg G (HBsAg decline > 1 $\log_{10}$ IU/mL). The baseline ALT, enrichment score of B cells, and intrahepatic B cell–related gene expression levels were compared among children with CHB who exhibited different degrees of HBeAg and HBsAg decline at week 48 of ETV treatment. When comparing HBeAg G group with HBeAg B group, we found that baseline ALT level was significantly higher in HBeAg G group than HBeAg B group (4.55×ULN vs. 2.03×ULN, P = 0.039) (Fig. 2A). And in HBeAg G group showed higher enrichment scores of hepatic activated B cell (-0.08 vs. -0.19, P = 0.042) and immature B cell (0.17 vs. 0.04, P = 0.019) than HBeAg B group (Fig. 2B). Besides, genes essential for B cell antigen receptor expression and function, such as MS4A1/CD20, CXCL13, and CD79A, were significantly upregulated in HBeAg G group compared to HBeAg B group (P < 0.05) (Fig. 2C). For the comparison of HBsAg G group to HBsAg B group, baseline ALT level tended to be higher in HBsAg G group, although without statistical significance (4.55×ULN vs. 2.08×ULN, P = 0.175, Fig. 2D). And enrichment scores of hepatic activated B cell (-0.08 vs. -0.12, P = 0.128) and immature B cell (0.14 vs. 0.11, P = 0.165) were also relatively higher in HBsAg G group than HBsAg B group but without statistical significance (Fig. 2E). B cell-related genes, such as MS4A1/CD20, BLK, and CXCL13, were significantly upregulated in HBsAg G group compared to HBsAg B group (P < 0.05, Fig. 2F).

Increased frequency and HBcAb production of peripheral circulating HBc-specific B cells in CHB children with elevated ALT levels

The above observations prompted us to investigate changes in HBV-specific B cells in CHB children. In this study, we focused on HBcAg-specific B cell (HBc-B) analysis rather than HBsAg-specific B cells, as HBc-B cells had been reported to be correlated with liver inflammation[28]. A total of 97 treatment-naïve children with chronic HBV infection were included as Cohort 2 for analyzing characteristics of circulating total B and HBc-B cells, including 49 with HBV DNA level > 10^8 IU/mL and normal ALT level (< 40 U/L) [IT phase], 40 with HBV DNA level > 10^6 IU/mL and elevated ALT level (1–5×ULN) [IA phase], and 8 with undetectable HBV DNA level and normal ALT level [IC phase]. Their detailed baseline parameters were shown in Table 2. Among the three groups, age and gender distribution did not differ ($P > 0.05$), while significant differences were observed in levels of HBsAg, HBV DNA, ALT, and AST ($P < 0.05$).

Table 2
Baseline characteristics of CHB children included in the analysis of peripheral total B and HBc-specific B cells

Variables	IT (n = 49)	IA (n = 40)	IC (n = 8)	*P* value
Age (years)	8.83(5.67-11.00)	7.72(3.67–11.02)	7.66(6.18-13.00)	0.330
Sex (boy, n (%))	26(53.1)	18(45.0)	4(50.0)	0.753
WBC (10^9/L)	6.11(5.23–7.45)	6.57(5.81–7.35)	6.03(5.66–6.74)	0.536
NEUT (10^9/L)	2.72(2.39–3.62)	2.85(2.31–3.74)	3.53(2.41–4.17)	0.621
LY (10^9/L)	2.79(2.03–3.36)	2.92(2.52–3.57)	2.32(1.98–2.78)	0.069
Mo(10^9/L)	0.30(0.24–0.38)	0.34(0.29–0.40)	0.25(0.21–0.30)	0.007
PLT (10^9/L)	266.00(236.00-303.00)	267.00(225.00-306.50)	318.00(244.50–350.00)	0.426
ALT (U/L)	24.00(18.00–31.00)	63.00(50.50–145.00)	21.50(19.00-26.50)	0.000
AST (U/L)	32.00(28.00-36.50)	55.00(45.00–80.00)	32.00(22.50–35.50)	0.000
TBIL (μmol/L)	8.00(5.65-11.00)	8.00(6.00-10.80)	8.75(7.20–13.50)	0.465
HBsAg (log_{10} IU/mL)	4.79(4.62–4.98)	4.29(3.89–4.69)	3.36(1.89–3.70)	0.000
HBV DNA (log_{10} IU/mL)	8.43(8.18–8.70)	7.97(6.89–8.46)	< LLOQ	0.000
Data are presented as the median and interquartile range (IQR), or numbers with percentages (%).				
IT, immune-tolerant phase; IA, immune-active phase; IC, immune-control phase; WBC, white blood cells; NEUT, neutrophils; LY, lymphocytes; Mo, monocytes; PLT, platelet; TBIL, total bilirubin; ALT, alanine aminotransferase; AST, aspartate transaminase; HBsAg, Hepatitis B surface antigen; HBV, hepatitis B virus; IU, international unit; LLOQ, lower limit of quantitation				

Flow cytometry gating for identification of peripheral circulating total B and HBc-B subpopulations was shown in **Supplementary Fig. 2**. As shown in Fig. 3A, there was no significant difference in the frequency of total B cells among children in different clinical phases (P > 0.05). However, the frequency of total memory B (B_{ME}) cells in children in the IA phase was significantly lower than that in the IT phase (2.19% vs. 2.95%, P = 0.019). In contrast, the frequency of HBc-B (IA vs. IT: 0.42% vs. 0.32%, P = 0.001; IA vs. IC: 0.42% vs. 0.28%, P = 0.007) and HBc-B_{ME} cells (IA vs. IT: 0.12% vs. 0.07%, P = 0.001; IA vs. IC: 0.12% vs. 0.08%, P = 0.024) in IA-phase children was significantly higher than those in both the IT and IC phases. Further analysis of memory B cell subsets revealed that the proportion of rest memory B (B_{RM}) cells (IA vs. IT: 15.39% vs. 19.29%, P = 0.006; IA vs. IC: 15.39% vs. 23.08%, P = 0.012) was significantly lower in children in the IA phase compared to those in the IT and IC phases (P < 0.05). Notably, the proportion of HBc-B_{AM} cells (IA vs. IT: 5.35% vs. 3.44%, P = 0.026; IA vs. IC: 5.35% vs. 0.61%, P = 0.000) was

significantly higher in IA-phase children than in those in the IT and IC phases. We also compared the percentages of three memory subsets between total B and HBc-B cells. Among the enrolled children, the proportions of B_{RM} (21.52% vs. 17.55%, P = 0.000) and B_{AM} subsets (3.91% vs. 1.95%, P = 0.000) were significantly higher, while the proportion of B_{ATM} subset (8.22% vs. 10.91%, P = 0.000) was significantly lower in HBc-B cells compared to those in total B cells (Fig. 3B). In summary, compared with total B cells, classical memory subsets (B_{RM} and B_{AM}) were enriched in HBcAg-specific B cells.

The capacity of IL-6 and IL-10 production of total B and HBc-B cells was further evaluated by in vitro stimulation. The results showed no significant differences were found among these CHB patients in different clinical phases (P > 0.05, **Supplementary Fig. 3**).

We also characterized HBc-B cell capacity to produce HBcAb, referred to as HBcAb-secreting spot-forming cells (HBcAb SFC). A significantly higher HBcAb SFC count was found in children in the IA phase than in those in the IT and IC phases (IA vs. IT: 120 vs. 53, P = 0.026; IA vs. IC: 120 vs. 11, P = 0.003), while no significant difference was observed between the IT and IC groups (P > 0.05). The levels of non-specific IgG SFCs showed no significant differences across the different clinical phases (P > 0.05, Fig. 3C). Furthermore, consistent with the trend of HBcAb SFC counts, serum HBcAb levels were significantly higher in IA-phase children compared to those in the IT and IC phases (IA vs. IT: 4.55 vs. 4.06 $\log_{10}$ IU/mL, P = 0.000; IA vs. IC: 4.55 vs. 3.19 $\log_{10}$ IU/mL, P = 0.000), while no significant difference was observed between the IT and IC groups (P > 0.05, Fig. 3D).

Correlation analysis among total B cells, HBc-B cells, their subsets, HBcAb SFC, and HBcAb levels was also analyzed (**Supplementary Fig. 4**). Notably, HBcAb SFC counts showed a strong positive correlation with the frequency of HBc-B_{ME} cells and serum HBcAb levels (RC were 0.659 and 0.728, respectively; both P < 0.05). Serum HBcAb levels showed a strong positive correlation with the frequency of HBc-B_{ME} cells (RC was 0.767, P < 0.05).

HBcAb SFC counts and HBcAb levels were significant positive correlated to degree of hepatic inflammation or ALT levels

Correlation analysis between HBc-B cells, their subsets, HBcAb SFC, HBcAb levels, and clinical index was further analyzed (Fig. 4A). Firstly, HBcAb SFC counts showed a significant positive correlation with liver inflammation grade (RC was 0.399, P < 0.05, Fig. 4A&4B). And CHB children with significant liver inflammation (G2-3 group) had higher HBcAb SFC counts (163 vs. 86, P = 0.036) than those with no-significant liver inflammation (G0-1 group) (Fig. 4C). Secondly, ALT or AST levels displayed a significant positive correlation with these HBc-B-related indicators except the frequency of HBc-B_{ATM} cells (P < 0.05, Fig. 4A**)**. Notably, ALT levels showed a strong positive correlation with serum HBcAb levels (RC was 0.643, P < 0.05), moderate positive correlations were observed with the frequency of HBc-B cells, HBc-B_{ME} cells, and HBcAb SFC counts (RC were 0.504, 0.574, and 0.533 respectively, both P < 0.05, Fig. 4A&4D). Comparison among children with different ALT levels [normal ALT (≤ 40 U/L), ALT 1–2×ULN (40–80 U/L), and ALT > 2×ULN (> 80 U/L)] showed that percentage of HBc-B (0.31% vs. 0.38% vs. 0.50%,

P = 0.000) or HBc-B_{ME} cells (0.33% vs. 0.51% vs. 1.25%, P = 0.000), HBcAb SFC counts (52 vs. 89 vs. 134, P = 0.002), and serum HBcAb levels (3.97 vs. 4.44 vs. 4.73 $\log_{10}$ IU/mL, P = 0.000) gradually increased with rising ALT levels (Fig. 4E). Furthermore, there was a negative correlation between HBsAg levels and the frequency of HBc-B_{ME} cells, HBcAb SFC counts, or serum HBcAb levels (P < 0.05, Fig. 4A**)**.

The number of HBcAb SFC and the quantitative level of serum HBcAb significantly decreased in CHB children during the 48-week follow-up period of ETV treatment

We also conducted a longitudinal analysis to explore the dynamic changes of HBc-B cells, memory subsets, HBcAb SFC and serum HBcAb levels in 17 CHB children (in Cohort 2) with ETV treatment. A gradual decline in ALT levels was observed during the 48-week follow-up period (Fig. 5A). A marked reduction in HBV DNA levels was observed at week 12, followed by a slower downward trend. The differences between baseline and each treatment follow-up time point were statistically significant (P < 0.05, Fig. 5A). Although no statistically significant differences in HBsAg or HBeAg levels were observed at any time point, a slow overall decreasing trend was noted (Fig. 5A).

The proportions of HBc-specific B cells and their memory subsets showed no significant changes during the 48-week course of treatment, but a slow downward trend was observed overall (Fig. 5B). Notably, HBcAb SFC counts showed a marked decrease at week 24 of treatment and subsequently remained stable. Statistically significant reductions were observed at weeks 24 and 48 compared to baseline (P < 0.05, Fig. 5C). In addition, a significant decline in serum HBcAb levels was observed over the follow-up period, with levels at week 24 and 48 being significantly lower than those at baseline (P < 0.05, Fig. 5D).

Higher peripheral HBc-B cells and HBcAb levels may be related to better efficacy of ETV antiviral therapy

Fourteen CHB children (in Cohort 2) with ETV antiviral therapy had completed 48 weeks of follow-up. The baseline, 12 and 48 weeks of follow-up characteristics of included patients were shown in **Supplementary table 2**. The baseline percentages of HBc-B cells and their subsets, HBcAb SFC counts, and serum HBcAb levels of included patients were shown in Fig. 6A. Treatment response was defined based on the reduction in HBeAg or HBsAg levels at week 12 or 48. As shown in Fig. 6A, patients were categorized into the following groups: the group of HBeAg B at 12W or 48W (HBeAg decline < 0.14 $\log_{10}$ s/co from baseline at week 12 of treatment or HBeAg decline < 0.45 $\log_{10}$ s/co from baseline at week 48 of treatment), the group of HBeAg G at 12W or 48W (HBeAg decline > 0.14 $\log_{10}$ s/co from baseline at week 12 of treatment or HBeAg decline > 0.45 $\log_{10}$ s/co from baseline at week 48 of treatment), the group of HBsAg B at 12W or 48W (HBsAg decline < 0.14 $\log_{10}$ IU/mL from baseline at week 12 of treatment or HBsAg decline < 0.45 $\log_{10}$ IU/mL from baseline at week 48 of treatment), and the group of HBsAg G at 12W or 48W (HBsAg decline > 0.14 $\log_{10}$ IU/mL from baseline at week 12 of treatment or HBsAg decline > 0.45 $\log_{10}$ IU/mL from baseline at week 48 of treatment).

The baseline parameters were compared among children with CHB who exhibited different degrees of HBeAg and HBsAg decline at week 12 and 48 of ETV treatment. We found that the proportion of baseline HBc-B cells (0.50% vs. 0.31%, P = 0.009) and HBc-B_{ME} cells (0.15% vs. 0.11%, P = 0.048) was significantly higher, while the proportion of HBc-B_{ATM} cells (12.57% vs. 4.52%, P = 0.006) was significantly lower in the group of HBeAg G at 12W (Fig. 6B). The proportion of baseline HBc-B cells (0.44% vs. 0.32%, P = 0.053), HBc-B_{ME} cells (0.14% vs. 0.11%, P = 0.053), HBcAb SFC counts (154 vs. 63, P = 0.071), and serum HBcAb levels (4.69 vs. 4.10 $\log_{10}$ IU/mL, P = 0.039) were also elevated in the group of HBeAg G at 48W (Fig. 6C). Although no statistically significant differences in the proportions of HBc-B cells and HBcAb levels were observed in patients who exhibited different degrees of HBsAg decline at week 12 and 48 of ETV treatment, the proportion of baseline HBc-B cells (0.49% vs. 0.32%, P = 0.179) and HBcAb SFC counts (162 vs. 77, P = 0.142) showed an increasing trend in the group of HBsAg G at 12W (Fig. 6D & 6E).

Discussion

Little is known about the intrahepatic immune profile in pediatric CHB patients with liver disease progression. We examined the intrahepatic transcriptomic profiles of 20 treatment-naïve children with CHB. Based on histological grading of liver inflammation, we identified 93 DEGs, including 55 upregulated and 38 downregulated genes. Subsequent GOBP enrichment analyses of the 55 upregulated DEGs revealed that GO terms such as B cell activation and B cell receptor signaling pathway played critical roles in the progression of hepatic inflammation in pediatric CHB. Therefore, we further assessed intrahepatic infiltration level of B cells. The results showed that enrichment scores of activated B cell and immature B cell were significantly higher in the G2-3 group. Besides, genes essential for B cell antigen receptor expression and function, such as MS4A1 (encoding CD20), CXCR5, and CD19, were significantly upregulated in the G2-3 group, and were also significantly positively correlated with ALT. Consistent with earlier observations reported in cohorts of adults with CHB, there was a notable increase in leukocyte infiltration in the livers of CHB patients, which was correlated with elevated serum ALT levels[19]. Hou et al. found that intrahepatic B cells and NK cells were elevated during the IA phase and the HBeAg-negative hepatitis phase[31]. Notably, PegIFN-α treatment increased the infiltration of monocytes and mast cells in both responders and non-responders but reduced the infiltration of CD8 + T cells and M1 macrophages. In contrast, B cell infiltration was increased only in responders[32]. In our study, higher baseline ALT level, enrichment scores of hepatic B cell, and transcriptomic expression of B cell–associated genes were correlated with a better virological response after 48-week ETV treatment in children with CHB.

Although accumulating evidence highlights the pivotal role of B cells in the control of HBV infection[33], investigations into B cell responses in HBV-infected individuals have been constrained by technical limitations, particularly in the analysis of antigen-specific B cells. The recent development of staining techniques utilizing fluorochrome-labeled HBs and HBc proteins has significantly advanced our understanding of the phenotypic and functional characteristics of antigen-specific B cells in CHB patients[28,34]. Studies have demonstrated that HBV-specific humoral immune responses in CHB patients were not universally dysfunctional. Notably, the frequency of peripheral HBcAg-specific B cells is

approximately ten times higher than that of HBsAg-specific B cells. Unlike HBsAg-specific B cells, HBcAg-specific B cells possess the capacity to effectively differentiate into antibody-secreting cells[28,34]. In this study, we firstly characterized the phenotypic features of both total circulating B cells and HBcAg-specific B cells in children with CHB. Our findings revealed that HBcAg-specific B cells were enriched in the classical memory subset. The frequency of HBcAg-specific B cells and their activated memory subsets were significantly elevated in IA-phase children, showing a progressive increase in parallel with rising ALT levels.

Previous cohort studies in adults with CHB have indicated that quantitative serum anti-HBc levels are correlated with ALT levels and demonstrate good predictive value for liver inflammation severity in treatment-naive patients[35,36]. However, the underlying mechanisms remain unclear, and reports on its application in pediatric cohorts are scarce.We found that both the HBcAb SFC counts and serum HBcAb levels were significantly elevated in children in the IA phase and showed a progressive increase with rising ALT levels. Furthermore, HBcAb SFC counts were correlated positively with intrahepatic inflammation grade, with significantly higher levels observed in CHB children with significant liver inflammation. Taken together, these findings suggested that the functional activation of HBcAg-specific B cells was closely linked to the progression of intrahepatic inflammation in pediatric CHB.

Subsequently, we aimed to explore the dynamic changes of HBc-B cell responses during 48-week ETV treatment. Although no consistent trends were observed in the frequencies of HBc-B cells or their memory subsets during ETV treatment, we found that both the HBcAb SFC counts and serum HBcAb levels declined significantly over the course of therapy. This decline may be associated with the resolution of hepatic inflammation during antiviral treatment. Recent studies in adult cohorts have shown that in HBeAg-positive patients, higher baseline levels of serum HBcAb were associated with increased rates of HBeAg seroconversion[37,38]. In our pediatric cohort, we evaluated the association between circulating HBc-B cells and their memory subsets, HBcAb levels, and the virological response to ETV therapy. Our findings suggested that higher baseline levels of HBc-B cells, HBc-B_{ME} cells, and HBcAb were correlated with more favorable treatment outcomes, especially for HBeAg decline.

Nevertheless, a causal relationship between HBcAg-specific humoral immune responses and CHB disease activity has yet to be established. Given that HBcAg is primarily expressed intracellularly within hepatocytes, HBcAg-specific B cells may have limited exposure to their cognate antigen prior to its release via cytotoxic T lymphocyte (CTL)-mediated lysis of infected hepatocytes[33]. This may indicate that HBcAg-specific B cell responses are not actively involved in the early inflammatory phase of hepatitis. Conversely, studies of HBV-induced acute liver failure (HBV-ALF) have revealed a different immune landscape. In patients with HBV-ALF, intrahepatic B cell gene signatures predominate, with marked infiltration of CD27 + MBCs that produce HBcAg-specific IgM and IgG antibodies, accompanied by complement deposition. Interestingly, intrahepatic T cell infiltration appears minimal, suggesting that in the context of HBV-ALF, B cells may engage HBcAg directly in a T cell–independent manner, leading to

antibody-dependent cell-mediated cytotoxicity (ADCC) and subsequent hepatocellular injury and necrosis[39,40].

In summary, our analysis of intrahepatic gene expression profiles in treatment-naïve children with CHB highlights a pivotal role for B cells in the progression of hepatic inflammation and the response to antiviral therapy. Further investigation demonstrated that the circulating HBc-B cell responses were closely associated with liver inflammation severity. Notably, higher baseline HBc-B cell responses were linked to more favorable antiviral treatment outcomes in pediatric CHB patients. These findings provide new insights into the immunological characteristics of pediatric CHB and offer potential guidance for optimizing the timing and strategies of antiviral therapy in clinical practice.

Abbreviations

Ab, antibody; Ag, antigen; ALT, alanine aminotranseferase; B_{AM}, activated memory B cells; B_{ATM}, atypical memory B cells; B_{ME}, memory B cells; B_{RM}, resting memory B cells; CHB, chronic hepatitis B; DCs, dendritic cells; DEGs, differentially expressed genes; ETV, entecavir; FBS, fetal bovine serum; FC, fold change; FDR, false discovery rate; G, grade of liver inflammation; GO-BP, gene ontology-biological process, GSEA, gene set enrichment analysis; HBc, hepatitis B core protein; HBcAb, hepatitis B core antibody; HBeAg, hepatitis B e antigen; HBsAg, hepatitis B surface antigen; HBV, hepatitis B virus; HCC, hepatocellular carcinoma; IA, the immune-active phase; IC, the immune-control phase; IFN, interferon; IQR, median and interquartile range; IT, the immune-tolerant phase; LLOQ, lower limit of quantitation; NK, natural kill cells; NUC, nucleos(t)ide analogue; PBMC, peripheral blood mononuclear Cells; qPCR, quantitative real-time polymerase chain reaction; S, stage of liver fibrosis; SFC, Ab-secreting spot-forming cell; ULN, upper limit of normal

Declarations

Authors’ contributions

Yingzhi Zhou: Conceptualization, Methodology, Investigation, Visualization, Writing - Original Draft. Jiangtao He, Huasi Wang, Kai Zhu, Jiaying Wu and Yunan Chang: Investigation, Visualization. Dachuan Cai and Hong Ren: Methodology, Investigation. Hongmei Xu and Min Chen: Conceptualization, Methodology, Writing - Review & Editing.

Conflict of interest statement

All authors declare no conflicts of interest.

Acknowledgements

This work was supported by Chongqing medical scientific research project (Joint project of Chongqing Health Commission and Science and Technology Bureau), China (2024MSXM024) (M.C.) This work was also supported by National Key Research and Development Program (2023YFC2308100) (H.X.), and Chongqing Postdoctoral Science Foundation Project (CSTB2022NSCQ - BHX0651) (Y.C.)

Data availability

The data used and/or analyzed during the current study are available from the corresponding author upon reasonable request.

References

1. Jeng WJ, Papatheodoridis GV, Lok A, Hepatitis. B Lancet. 2023;401:1039–52.
2. Polaris OC. Global prevalence, treatment, and prevention of hepatitis B virus infection in 2016: a modelling study. Lancet Gastroenterol Hepatol. 2018;3:383–403.
3. Paganelli M, Stephenne X, Sokal EM. Chronic hepatitis B in children and adolescents. J Hepatol. 2012;57:885–96.
4. Zhu SS, Dong Y, Xu ZQ, Wang LM, Chen DW, Gan Y, et al. A retrospective study on HBsAg clearance rate after antiviral therapy in children with HBeAg-positive chronic hepatitis B aged 1–7 years. Zhong Hua Gan Zang Bing Za Zhi. 2016;24:738–43.
5. Bortolotti F, Guido M, Bartolacci S, Cadrobbi P, Crivellaro C, Noventa F, et al. Chronic hepatitis B in children after e antigen seroclearance: final report of a 29-year longitudinal study. Hepatology. 2006;43:556–62.
6. Wen WH, Chang MH, Hsu HY, Ni YH, Chen HL. The development of hepatocellular carcinoma among prospectively followed children with chronic hepatitis B virus infection. J Pediatr. 2004;144:397–9.
7. You H, Wang F, Li T, Xu X, Sun Y, Nan Y, et al. Guidelines for the Prevention and Treatment of Chronic Hepatitis B (version 2022). J Clin Transl Hepatol. 2023;11:1425–42.
8. Khanam A, Chua JV, Kottilil S. Immunopathology of Chronic Hepatitis B Infection: Role of Innate and Adaptive Immune Response in Disease Progression. Int J Mol Sci. 2021;22:5497.
9. Zhang Z, Chen D, Yao J, Zhang H, Jin L, Shi M, et al. Increased infiltration of intrahepatic DC subsets closely correlate with viral control and liver injury in immune active pediatric patients with chronic hepatitis B. Clin Immunol. 2007;122:173–80.
10. Zhou Y, He Y, Chang Y, Peng X, Zhao R, Peng M, et al. The Characteristics of Natural Killer Cells and T Cells Vary With the Natural History of Chronic Hepatitis B in Children. Front Pediatr. 2021;9:736023.
11. McLane LM, Abdel-Hakeem MS, Wherry EJ. CD8 T Cell Exhaustion During Chronic Viral Infection and Cancer. Annu Rev Immunol. 2019;37:457–95.

12. Takahama S, Yoshio S, Masuta Y, Murakami H, Sakamori R, Kaneko S, et al. Hepatitis B surface antigen reduction is associated with hepatitis B core-specific CD8 + T cell quality. Front Immunol. 2023;14:1257113.
13. Kim JH, Ghosh A, Ayithan N. Circulating serum HBsAg level is a biomarker for HBV-specific T and B cell responses in chronic hepatitis B patients. Sci Rep 1835;2020:10.
14. Rivino L, Le Bert N, Gill US, Kunasegaran K, Cheng Y, Tan DZ, et al. Hepatitis B virus-specific T cells associate with viral control upon nucleos(T)Ide-analogue therapy discontinuation. J Clin Invest. 2018;128:668–81.
15. Le Bert N, Salimzadeh L, Gill US, Dutertre CA, Facchetti F, Tan A, et al. Comparative characterization of B cells specific for HBV nucleocapsid and envelope proteins in patients with chronic hepatitis B. J Hepatol. 2020;72:34–44.
16. Le Bert N, Gill US, Hong M, Kunasegaran K, Tan DZM, Ahmad R, et al. Effects of hepatitis B surface antigen on virus-specific and global T cells in patients with chronic hepatitis B virus infection. Gastroenterology. 2020;159:652–64.
17. Aliabadi E, Urbanek-Quaing M, Maasoumy B, Bremer B, Grasshoff M, Li Y, et al. Impact of HBsAg and HBcrAg levels on phenotype and function of HBV-specific T cells in patients with chronic hepatitis B virus infection. Gut. 2022;71:2300–12.
18. Kennedy PTF, Sandalova E, Jo J, Gill U, Ushiro-Lumb I, Tan AT, et al. Preserved T-cell function in children and young adults with immune-tolerant chronic hepatitis B. Gastroenterology. 2012;143:637–45.
19. Montanari NR, Ramírez R, Aggarwal A, van Buuren N, Doukas M, Moon C, et al. Multi-parametric analysis of human livers reveals variation in intrahepatic inflammation across phases of chronic hepatitis B infection. J Hepatol. 2022;77:332–43.
20. Van Buuren N, Ramirez R, Turner S, Chen D, Suri V, Aggarwal A, et al. Characterization of the liver immune microenvironment in liver biopsies from patients with chronic HBV infection. JHEP Rep. 2021;4:100388.
21. Zhang JW, Lai RM, Wang LF, Wang SL, Xue HX, Li C, et al. Varied immune responses of HBV-specific B cells in patients undergoing pegylated interferon-alpha treatment for chronic hepatitis B. J Hepatol. 2024;81:960–70.
22. He T, Chen M, Liu M, Zhang L, Sun H, Zhang L et al. Twenty-four-week anti-PD-1 antibody regimen promoted HBsAg reduction and concurrently enhanced HBV-specific T cell responses in patients with chronic hepatitis B. Gut 2025:gutjnl–2025.
23. Yuen MF, Seto WK, Fung J, Wong DK, Yuen JC, Lai CL. Three years of continuous entecavir therapy in treatment-naïve chronic hepatitis B patients: VIRAL suppression, viral resistance, and clinical safety. Am J Gastroenterol. 2011;106:1264–71.
24. Yao GB, Ren H, Xu DZ, Zhou XQ, Jia JD, Wang YM, et al. Virological, serological and biochemical outcomes through 3 years of entecavir treatment in nucleoside-naive Chinese chronic hepatitis B patients. J Viral Hepat. 2010;17(Suppl 1):51–8.

25. Jonas MM, Chang MH, Sokal E, Schwarz KB, Kelly D, Kim KM, et al. Randomized, controlled trial of entecavir versus placebo in children with hepatitis B envelope antigen-positive chronic hepatitis B. Hepatology. 2016;63:377–87.
26. Zhang Z, Zhang H, Chen D, Yao J, Fu J, Jin L, et al. Response to interferon-alpha treatment correlates with recovery of blood plasmacytoid dendritic cells in children with chronic hepatitis B. J Hepatol. 2007;47:751–9.
27. Carey I, D'Antiga L, Bansal S, Longhi MS, Ma Y, Mesa IR, et al. Immune and viral profile from tolerance to hepatitis B surface antigen clearance: a longitudinal study of vertically hepatitis B virus-infected children on combined therapy. J Virol. 2011;85:2416–28.
28. Vanwolleghem T, Groothuismink ZMA, Kreefft K, Hung M, Novikov N, Boonstra A. Hepatitis B core-specific memory B cell responses associate with clinical parameters in patients with chronic HBV. J Hepatol. 2020;73:52–61.
29. Love MI, Huber W, Anders S. Moderated estimation of fold change and dispersion for RNA-seq data with DESeq2. Genome Biol. 2014;15:550.
30. Bindea G, Mlecnik B, Tosolini M, Kirilovsky A, Waldner M, Obenauf AC, et al. Spatiotemporal dynamics of intratumoral immune cells reveal the immune landscape in human cancer. Immunity. 2013;39:782–95.
31. Hou J, Brouwer WP, Kreefft K, Gama L, Price SL, Janssen HLA, et al. Unique intrahepatic transcriptomics profiles discriminate the clinical phases of a chronic HBV infection. PLoS ONE. 2017;12:e179920.
32. Li N, Yu K, Dong M, Wang J, Yang F, Zhu H, et al. Intrahepatic transcriptomics reveals gene signatures in chronic hepatitis B patients responded to interferon therapy. Emerg Microbes Infect. 2022;11:1876–89.
33. Vanwolleghem T, Adomati T, Van Hees S, Janssen HLA. Humoral immunity in hepatitis B virus infection: Rehabilitating the B in HBV. JHEP Rep. 2022;4:100398.
34. Le Bert N, Salimzadeh L, Gill US, Dutertre CA, Facchetti F, Tan A, et al. Comparative characterization of B cells specific for HBV nucleocapsid and envelope proteins in patients with chronic hepatitis B. J Hepatol. 2020;72:34–44.
35. Song LW, Liu PG, Liu CJ, Zhang TY, Cheng XD, Wu HL, et al. Quantitative hepatitis B core antibody levels in the natural history of hepatitis B virus infection. Clin Microbiol Infect. 2015;21:197–203.
36. Li MR, Lu JH, Ye LH, Sun XL, Zheng YH, Liu ZQ, et al. Quantitative hepatitis B core antibody level is associated with inflammatory activity in treatment-naïve chronic hepatitis B patients. Med (Baltim). 2016;95:e4422.
37. Xu JH, Song LW, Li N, Wang S, Zeng Z, Si CW, et al. Baseline hepatitis B core antibody predicts treatment response in chronic hepatitis B patients receiving long-term entecavir. J Viral Hepat. 2017;24:148–54.
38. Fan R, Sun J, Yuan Q, Xie Q, Bai X, Ning Q, et al. Baseline quantitative hepatitis B core antibody titre alone strongly predicts HBeAg seroconversion across chronic hepatitis B patients treated with

peginterferon or nucleos(t)ide analogues. Gut. 2016;65:313–20.

39. Chen Z, Diaz G, Pollicino T, Zhao H, Engle RE, Schuck P, et al. Role of humoral immunity against hepatitis B virus core antigen in the pathogenesis of acute liver failure. Proc Natl Acad Sci U S A. 2018;115:E11369–78.

40. Chen Z, Shen CH, Engle RE, Zamboni F, Kwong PD, Purcell RH, et al. Next-generation sequencing of the intrahepatic antibody repertoire delineates a unique B-cell response in HBV-associated acute liver failure. J Viral Hepat. 2020;27:847–51.

Figures

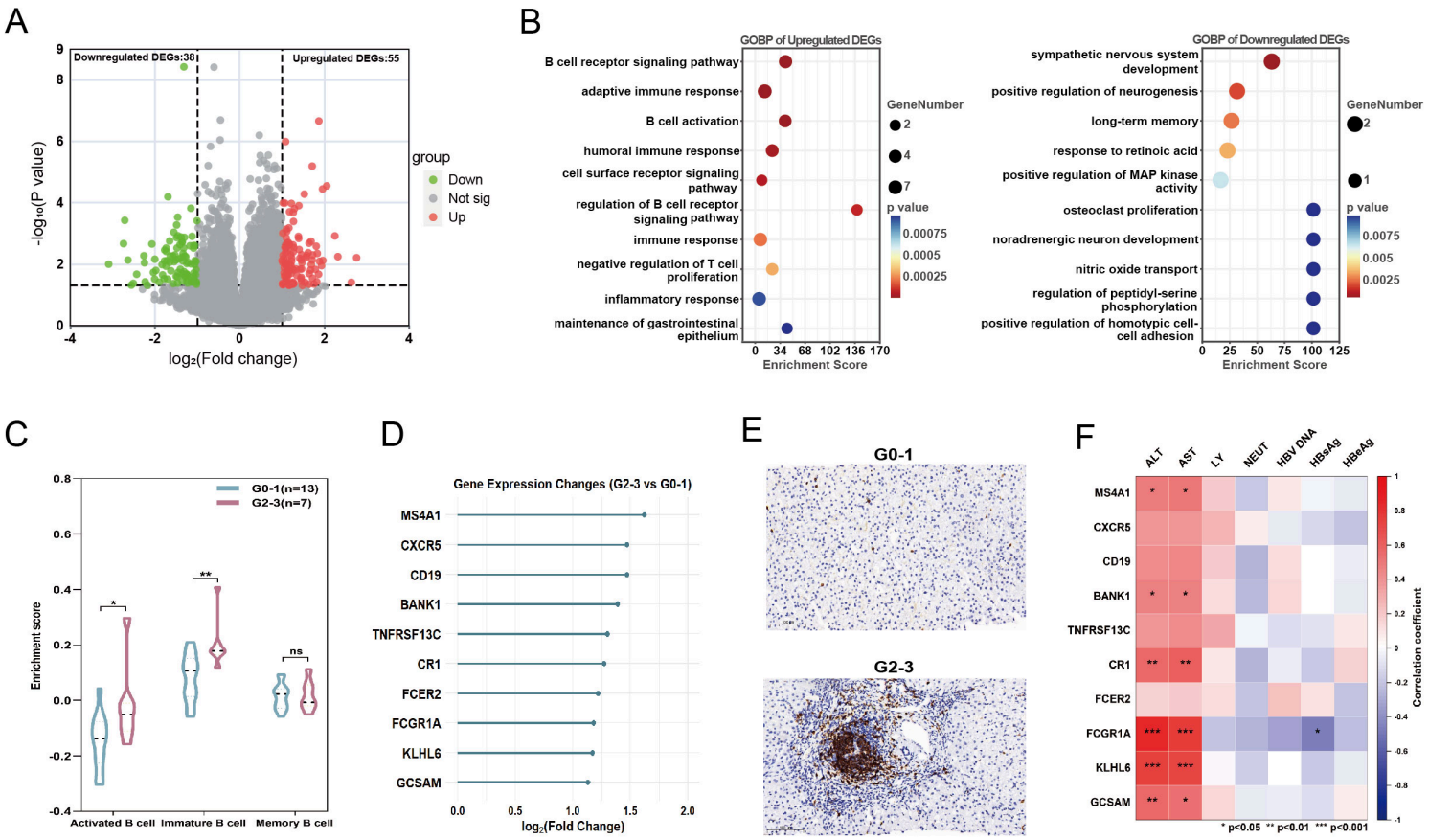


Figure 1

B cell activation-related pathways and genes were enriched in livers from CHB children with significant liver inflammation

A, Volcano plot for the differentially expressed genes (DEGs) of liver transcriptome of moderate-to-severe liver inflammation (G2-3) versus no-activity or minimal liver inflammation (G0-1).

B, Bubble plot showing the top 10 significantly enriched GO terms of upregulated or downregulated DEGs (G2-3 vs. G0-1) for biological process (GO-BP).

C, Immune infiltration analysis using ssGSEA demonstrated a higher enrichment score of B cells in the G2-3 group.

D, Relative mRNA expression (fold change) of significantly upregulated B cell-related genes.

E, Representative images of immunohistochemical staining (brown) of MS4A1 (CD20, marker for B lymphocytes) in G2-3 vs. G0-1 group.

F, Correlation analysis between significantly upregulated B cell-related genes and clinical indicators.

CHB, chronic hepatitis B; G, grade of liver inflammation; GO-BP, gene ontology-biological process, GSEA, gene set enrichment analysis

*, p <0.05; **, p < 0.01; ***, p < 0.001.

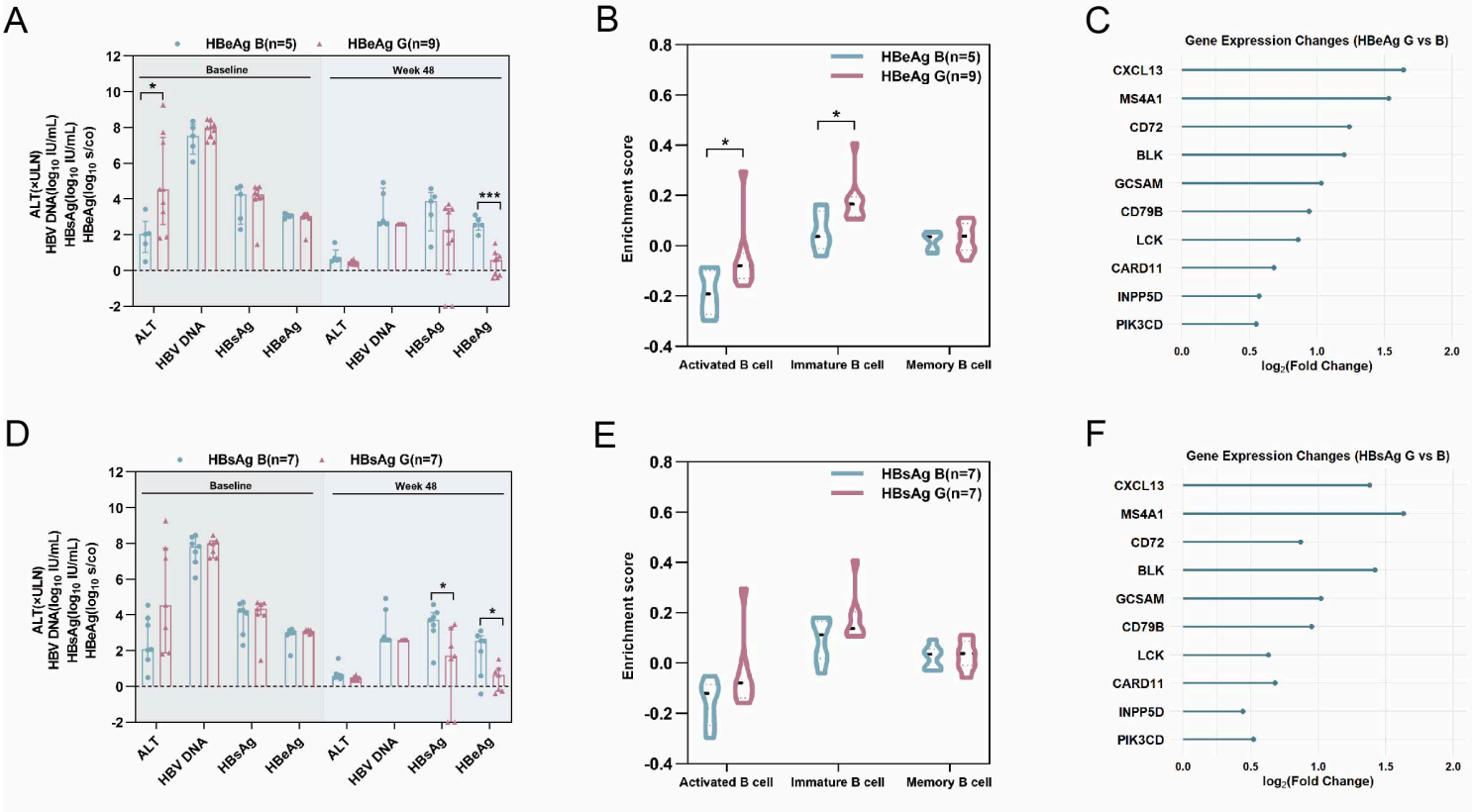


Figure 2

Higher hepatic active B-cell infiltration and B cell-related gene expression in CHB children with a better antiviral response

A, Comparison of parameters at baseline or week 48 after antiviral therapy between CHB children in the HBeAg B and HBeAg G group.

B, Comparison of enrichment score of hepatic B cells between HBeAg B and HBeAg G group.

C, Relative mRNA expression of B cell-related genes (fold change) was upregulated in HBeAg G group compared to HBeAg B group.

D, Comparison of parameters at baseline or week 48 after antiviral therapy between CHB children in the HBsAg B and HBsAg G group.

E, Comparison of enrichment score of hepatic B cells between HBsAg B and HBsAg G group.

F, Relative mRNA expression of B cell-related genes (fold change) was upregulated in HBsAg G group.

HBeAg B group, HBeAg declined < 1 log_{10} s/co at week 48 vs. Baseline; HBeAg G group, HBeAg declined >1 log_{10} s/co at week 48 vs. Baseline; HBsAg B group, HBsAg declined < 1 log_{10} IU/mL at week 48 vs. Baseline; HBsAg G group, HBsAg declined >1 log_{10} IU/mL at week 48 vs. Baseline. ULN, upper limit of normal (40U/L).

*, p < 0.05; **, p < 0.01.

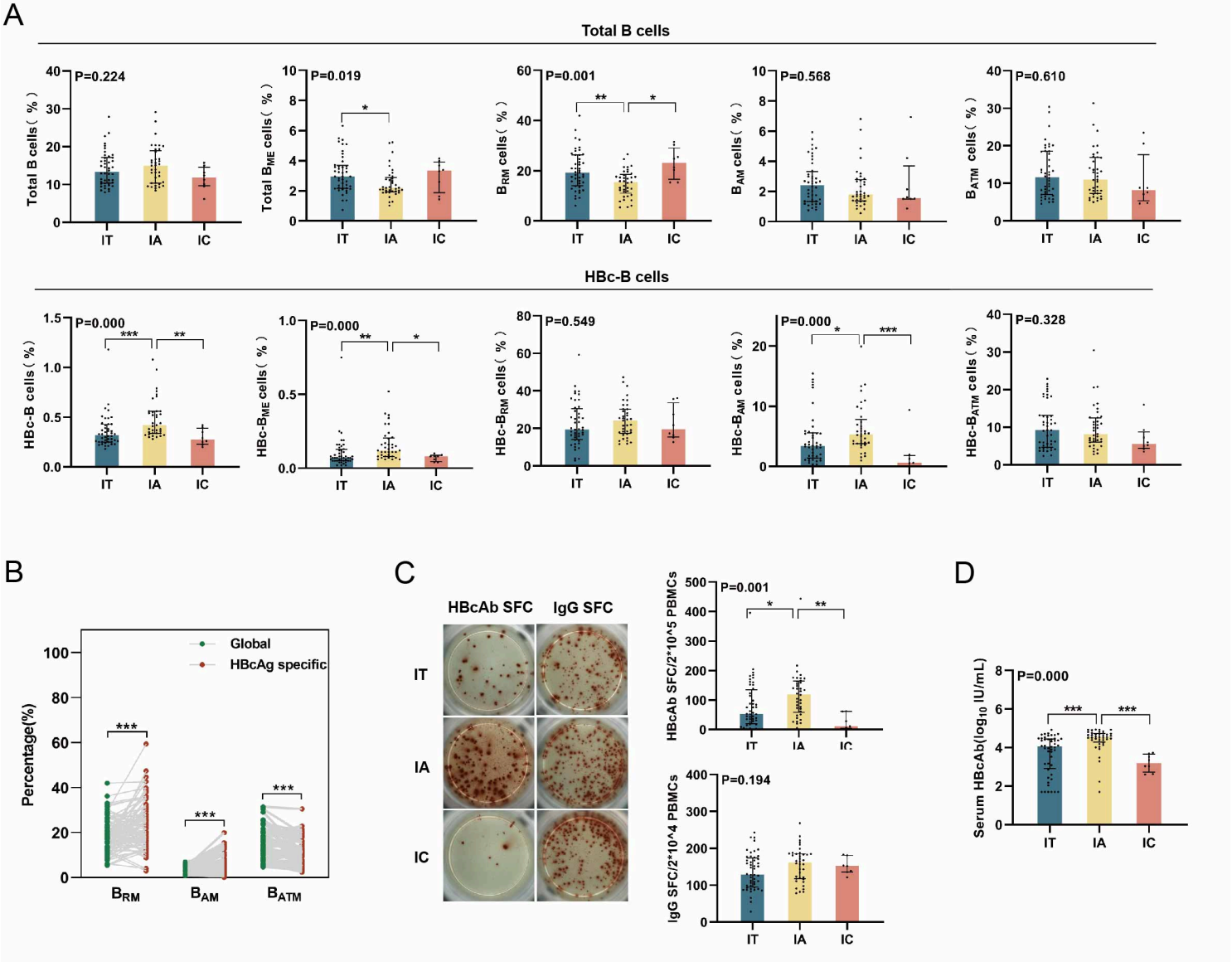


Figure 3

Assays of peripheral circulating total B and HBc-specific B cells in CHB children

A, Comparison of percentage of circulation total B cells, HBc-specific B cells, and their subsets in CHB children during immune-tolerant (IT), immune-active (IA), or immune-clearance (IC) phase. Subsets included memory B (B_{ME}) cells, resting memory B (B_{RM}) cells, activated memory B (B_{AM}) cells, and atypical memory B (B_{ATM}) cells.

B, Higher percentages of B_{RM} and B_{AM}, while lower percentages of B_{ATM} in HBc-specific B cells than those in total B cells.

C, Higher number of HBc antibody spot-forming cells (SFC) in CHB children in the IA phase.

D, Higher level of serum HBcAb in CHB children in the IA phase.

*, $p < 0.05$; **, $p < 0.01$; ***, $p < 0.001$.

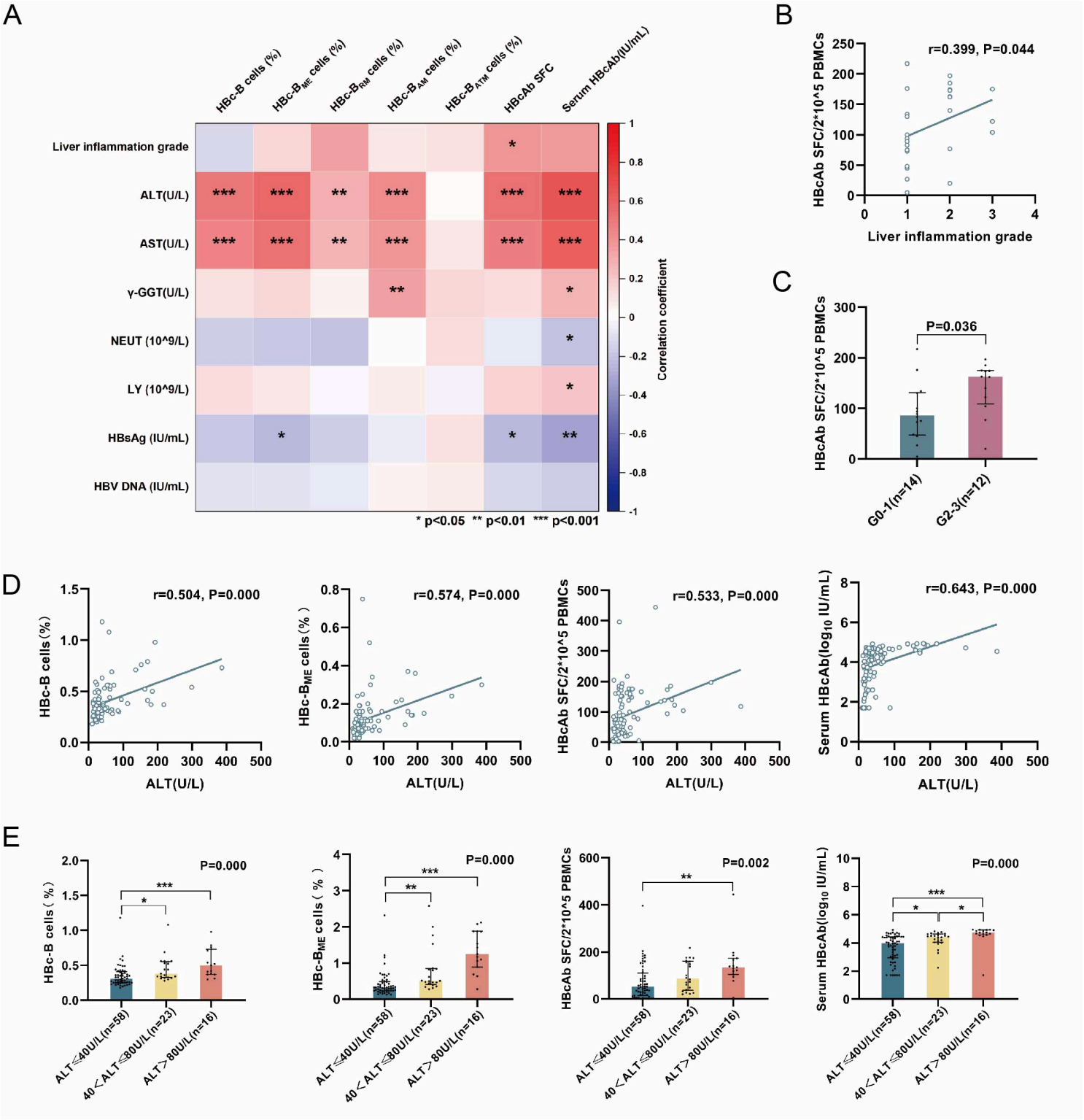


Figure 4

Correlation analysis among peripheral HBc-B cells and liver inflammation, or blood laboratory parameters

A, Correlation analysis among phenotype and function of HBc-B cells and hepatic and blood parameters.

B, Scatterplots displayed the significant correlations between HBc-B cells and liver inflammation grade.

C, Comparison of HBc-B cells between CHB children with moderate-to-severe liver inflammation (G2-3) and no-activity or minimal liver inflammation (G0-1).

D, Scatterplots displayed the significant correlations between HBc-B cells and ALT.

E, Comparison of HBc-B cells among CHB children with normal ALT (≤ 40 U/L), ALT 1-2×ULN (40-80 U/L), and ALT > 2×ULN (>80 U/L).

*, $p < 0.05$; **, $p < 0.01$; ***, $p < 0.001$.

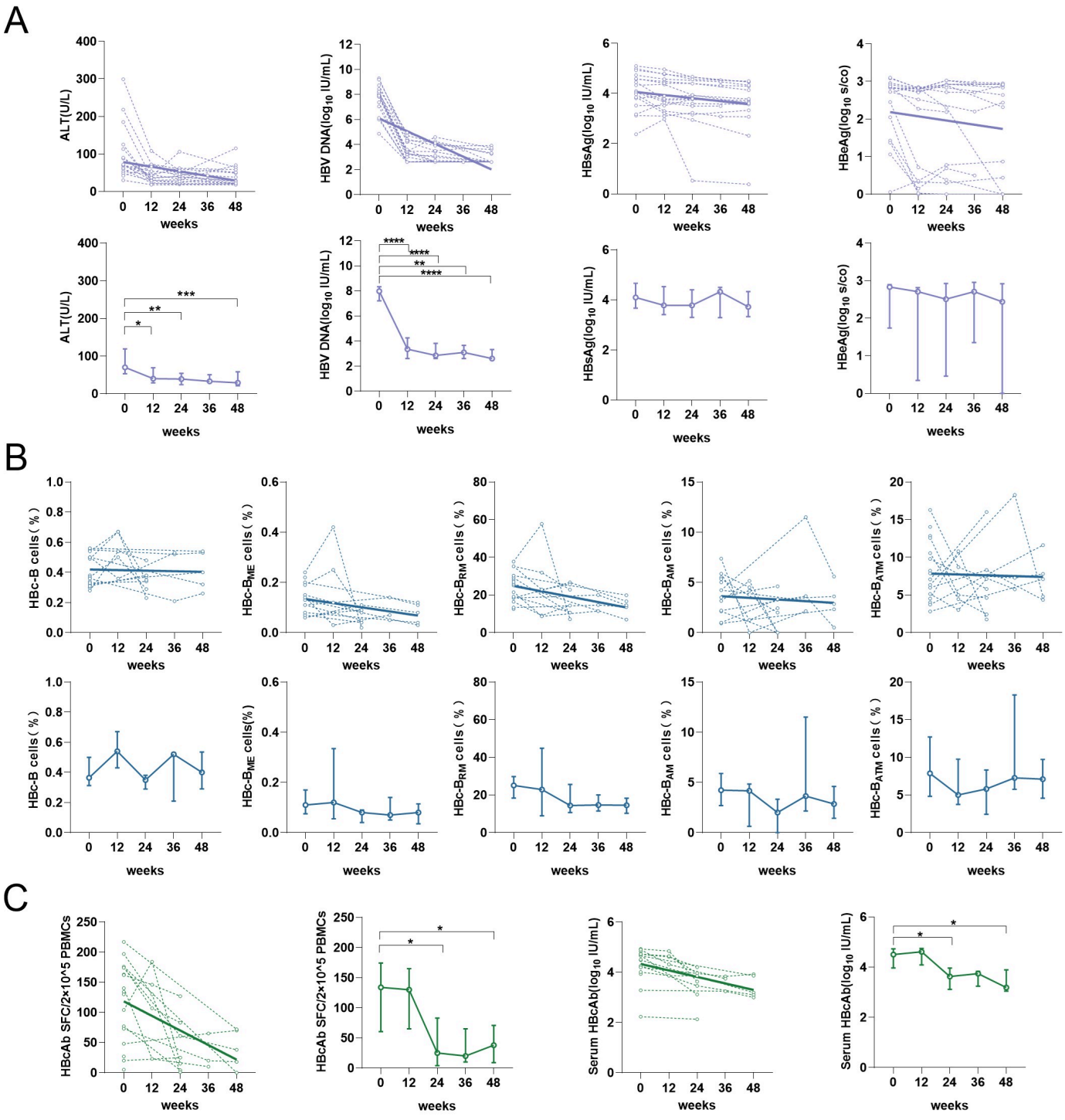


Figure 5

Dynamic changes in HBc-B cells during 48 weeks of ETV treatment

A, Individual patient trajectories and trendline (the upper panel), and overall dynamics at each timepoint (the lower panel) of ALT, HBV DNA, HBsAg, and HBeAg levels.

B, Individual patient trajectories and trendline (the upper panel), and overall dynamics at each timepoint (the lower panel) of the frequency of HBc-B cells and their memory subsets. Subsets included memory B cells (HBc-B_{ME}), resting memory B cells (HBc-B_{RM}), activated memory B cells (HBc-B_{AM}), and atypical memory B cells (HBc-B_{ATM}).

C and D, Individual patient trajectories and trendline (the left plot), and overall dynamics at each timepoint (the right plot) of the HBcAb SFC counts (C) and serum HBcAb quantitative level (D).

*, $p < 0.05$; **, $p < 0.01$; ***, $p < 0.001$; ****, $p < 0.0001$.

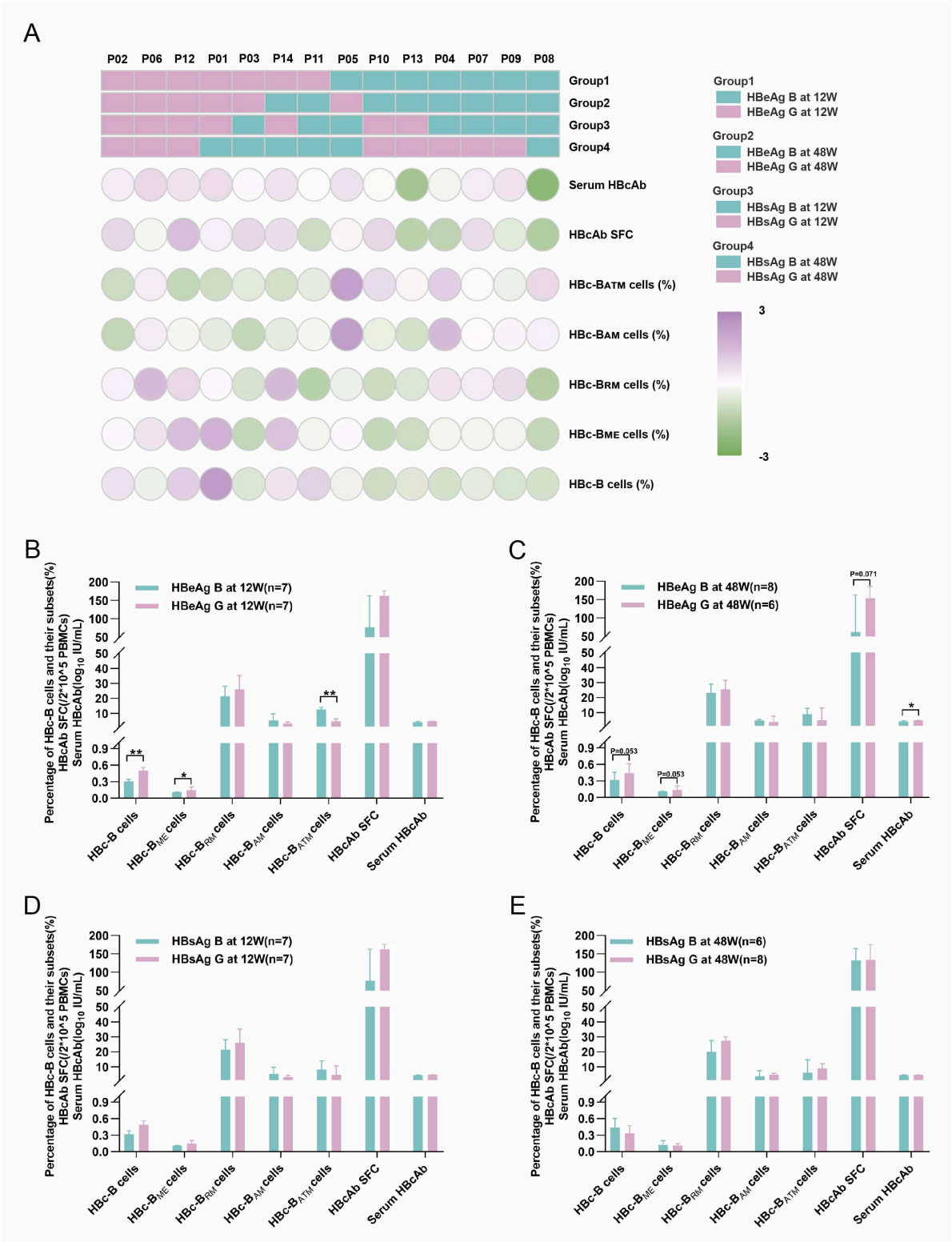


Figure 6

Relatively higher peripheral HBc-B cells and HBcAb levels in CHB children with better efficacy of Entecavir antiviral therapy

A, Heatmap showing baseline HBc-B cells and HBcAb levels of 14 CHB children receiving anti-viral therapy with Entecavir.

B, Comparisons of baseline HBc-B cells and HBcAb levels between CHB children with HBeAg declined < 0.14 $\log_{10}$ s/co (HBeAg B at 12W) and HBeAg declined > 0.14 $\log_{10}$ s/co (HBeAg G at 12W) from baseline at week 12 of treatment.

C, Comparisons of baseline HBc-B cells and HBcAb levels between CHB children with HBeAg declined < 0.45 $\log_{10}$ s/co (HBeAg B at 48W) and HBeAg declined > 0.45 $\log_{10}$ s/co (HBeAg G at 48W) from baseline at week 48 of treatment.

D, Comparisons of baseline HBc-B cells and HBcAb levels between CHB children with HBsAg declined < 0.14 $\log_{10}$ IU/mL (HBsAg B at 12W) and HBsAg declined > 0.14 $\log_{10}$ IU/mL (HBsAg G at 12W) from baseline at week 12 of treatment.

E, Comparisons of baseline HBc-B cells and HBcAb levels between CHB children with HBsAg declined < 0.45 $\log_{10}$ IU/mL (HBsAg B at 48W) and HBsAg declined > 0.45 $\log_{10}$ IU/mL (HBsAg G at 48W) from baseline at week 48 of treatment.

*, $p < 0.05$; **, $p < 0.01$.

Supplementary Files

This is a list of supplementary files associated with this preprint. Click to download.

- SupplementalFiles.docx
- coverletter.docx